Applied Surface Science 428 (2018) 118–123

Contents lists available at ScienceDirect

Applied Surface Science

journal homepage: www.elsevier.com/locate/apsusc

Full Length Article

Comparison of standard DFT and Hubbard-DFT methods in structural and electronic properties of TiO_2 polymorphs and H-titanate ultrathin sheets for DSSC application

Estefania German[a,b,*], Ricardo Faccio[b,*], Alvaro W. Mombrú[b]

[a] Instituto de Física del Sur (IFISUR), Departamento de Física, Universidad Nacional del Sur (UNS), CONICET, Av. L. N. Alem 1253, B8000CPB, Bahía Blanca, Argentina
[b] Centro NanoMat-DETEMA, Facultad de Química, Universidad de la República, Uruguay

ARTICLE INFO

Article history:
Received 10 March 2017
Received in revised form 1 September 2017
Accepted 17 September 2017

Keywords:
TiO_2
Hydrogen titanate
Surfaces
DFT
DSSC
Hubbard

ABSTRACT

The structural and electronic properties of several TiO_2 polymorphs and hydrogen titanate surfaces are modeled and studied by density functional theory (DFT). By implementing the Hubbard parameter "U" in our calculations more realistic results of electronic properties are obtained, paying with a small deviation in geometric optimization. Lattice parameters difference is found to be less than 6.2%, as well as some changes in surface energy are found, but the reactivity tendency of surfaces is maintained. Calculated work function is less energetic for faces (001) for anatase, (101) for rutile and (001) for TiO_2-B.

1. Introduction

Titanium dioxide has become the most studied photocatalytic material because it is abundant, relatively cheap and not easy to dissociate or to degrade [1]. In the past years, the number of TiO_2 surfaces studies have increased. We can find several experimental [2,3] and theoretical [4–7] studies. The most abundant TiO_2 forms are rutile, anatase and brookite [8–11]. TiO_2-B polymorph gained more attention due to its applications like rechargeable lithium ion batteries [12,13], dye sensitized solar cells (DSSCs) [14,15] and supercapacitors [16]. On the other hand, hydrogen titanate has become a compound of interest: it was synthesized as nanotubes and characterized by several authors due to their promising properties and applications [17–20]. Besides, it was modeled as a bulk material starting from crystallographic data [21,22]. In spite of all this, there are still doubts about its right crystal structure, which is necessary to understand its potential properties, giving that it is a promising surface for DSSC application [23–25]. As it was expressed above, our interest in titanium surfaces lies in its potential application in DSSCs, so the understanding of these surfaces will make easier the study of dye molecules adsorption on them.

Although in literature we can find several theoretical and experimental studies regarding anatase and rutile and in a lesser extent regarding TiO_2-B polymorph [26–29], the knowledge about hydrogen titanate is scarse [23–25,30–33]. We have performed a theoretical study using the first principle method called DFT, to characterize structural and electronic properties of these TiO_2 polymorphs and hydrogen titanate surfaces.

Due to the increase in computational potential, DFT has become the best method for many-body approaches calculation, despite its deficit in processing materials containing partially-filled *d* and *f* shells. When transition metal oxides are the subject under study, the problem of underestimation of band gap for insulators leads to untrustworthy descriptions of defect states located within the band gap [34–38]. For the study of electronic properties in these transition metal oxides, it is needed a method or approximation to correct the shortfall for strongly correlated metal oxides. DFT + U method (LDA + U or GGA + U) is more efficient in the calculation than hybrid functional methods, however some parameters need to be fitted and introduced [37,39,40]. This method separates the electrons in two groups, the fully occupied orbitals, which are treated with DFT approach, and partially filled localized orbitals, treated by the Hubbard model, the latter with strong electron–electron correlations. However we can find in literature the development of general pro-

* corresponding authors.
E-mail addresses: egerman@uns.edu.ar, estefaniagerman@hotmail.com (E. German), rfaccio@fq.edu.uy (R. Faccio).

http://dx.doi.org/10.1016/j.apsusc.2017.09.141
0169-4332/

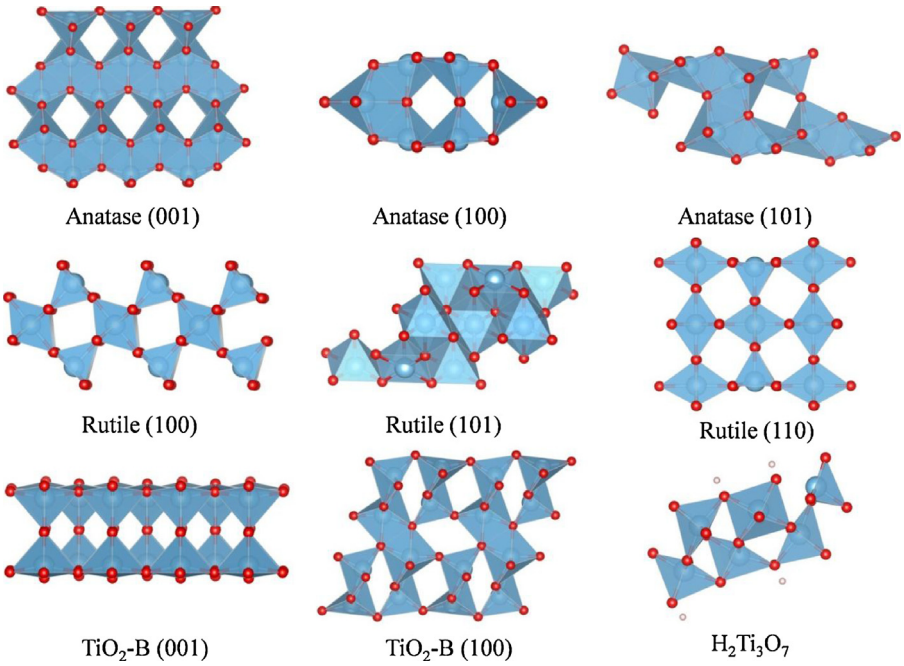

Fig. 1. Optimized geometries of studied surfaces calculated using DFT + U, namely, anatase (001), (100) and (101) where U = 8 eV, rutile (100), (101) and (110) where U = 10 eV, TiO_2-B (001) and (100) where U = 4 eV and hydrogen titanate (100) where U = 5 eV.

Table 1
Comparison of lattice parameters for the studied surfaces calculated by DFT and DFT + U methods.

	Lattice parameters					
	DFT			DFT + U		
Surfaces	a(Å)	b(Å)	c(Å)	a(Å)	b(Å)	c(Å)
Anatase (001)	3.72	3.72	28.18	3.78	3.79	27.21
Anatase (100)	9.48	7.37	13.06	9.59	7.59	12.55
Anatase (101)	15.62	3.72	10.30	15.25	3.80	10.51
Rutile (100)	8.74	13.97	19.13	8.99	14.24	18.24
Rutile (101)	4.56	5.44	16.28	4.59	5.56	15.93
Rutile (110)	2.94	6.45	19.36	3.03	6.65	18.23
TiO_2-B (001)	11.77	11.04	19.52	11.86	11.22	19.10
TiO_2-B (100)	12.94	7.49	26.54	13.06	7.60	25.98
$H_2Ti_3O_7$	9.40	3.71	19.30	9.38	3.82	18.81

Table 2
Relaxed Ti-O surface bond lengths in Å calculated using DFT and DFT + U method.

Surfaces	Superficial Ti-O (Å)	Inner Ti-O (Å)
Anatase (001) – DFT	2.13, 1.92	1.94
Anatase (001) – DFT + U	1.95	2.02
Anatase (100) – DFT	1.93, 1.78	2.21, 1.86
Anatase (100) – DFT + U	1.98, 1.82	2.20, 1.92
Anatase (101) – DFT	1.84, 1.91, 1.96	2.06, 2.13
Anatase (101) – DFT + U	1.87, 1.90, 1.99	1.89, 2.07
Rutile (100) – DFT	1.85	2.04
Rutile (100) – DFT + U	1.90	2.05
Rutile (101) – DFT	1.80, 1.92	1.97, 2.13
Rutile (101) – DFT + U	1.90, 1.93	2.06, 2.08
Rutile (110) – DFT	1.80, 1.92	1.85, 2.00
Rutile (110) – DFT + U	1.90, 1.97	1.93, 2.10
TiO_2-B (001) – DFT	1.83, 1.93	1.81
TiO_2-B (001) – DFT + U	1.85, 1.95	1.84
TiO_2-B (100) – DFT	1.81, 1.95	1.96
TiO_2-B (100) – DFT + U	1.84, 1.94	1.99
$H_2Ti_3O_7$ – DFT	2.03, 1.90, 2.28, 1.64	1.95, 1.89, 2.00
$H_2Ti_3O_7$ – DFT + U	2.10, 1.94, 2.22, 1.67	2.00, 1.96, 2.06

tocols attempting to avoid resorting to empirical parameters fitting for LDA + U method [41,42]. But in our case, we decided to study how the selection of U_{eff} affects the electronic properties of the studied systems.

Here, we present a comparison study of how the addition of Hubbard term in the calculation affects the structural and electronic properties of titanium oxide polymorphs and hydrogen titanate surfaces. We have studied anatase (001), (100) and (101), rutile (100), (101) and (110), TiO_2-B (001) and (100) and hydrogen titanate ($H_2Ti_3O_7$). Lattice parameters, bond lengths, surface energy, band gap, DOS curves and work function have been evaluated in order to better understand the behavior and applications of these surfaces in solar cells.

2. Computational method

All calculations were carried out within the frame of the density functional theory (DFT) [43] using the Vienna Ab-Initio Simulation Package (VASP) [44] which employs a plane-wave basis set and a periodic supercell method. The projector augmented wave (PAW) method [45,46] was used to account for the electron–ion core interaction, using the Perdew-Burke-Ernzerhof (PBE) as the generalized gradient approximation (GGA) [47] for the exchange-correlation term.

In transition metal oxides, the GGA approach gets a self-interaction error, which affects the electronic structure. In order to

Table 3
Equivalent surface energies (J/m^2) and energy gaps (eV) for the studied surfaces, comparison of DFT and DFT + U calculation.

	Surface Energy (J/m^2)		Energy Gap (eV)	
Surfaces	DFT	DFT + U	DFT	DFT + U
Anatase (001)	0.75	0.42	2.09	2.32
Anatase (100)	0.55	0.61	2.23	2.76
Anatase (101)	0.29	0.28	2.83	3.38
Rutile (100)	0.61	0.60	2.03	3.06
Rutile (101)	1.01	0.90	1.89	2.65
Rutile (110)	0.58	0.27	1.29	2.06
TiO_2-B (001)	0.20	0.18	2.59	3.06
TiO_2-B (100)	0.52	0.36	2.85	2.98
$H_2Ti_3O_7$	0.20	0.15	1.82	2.31

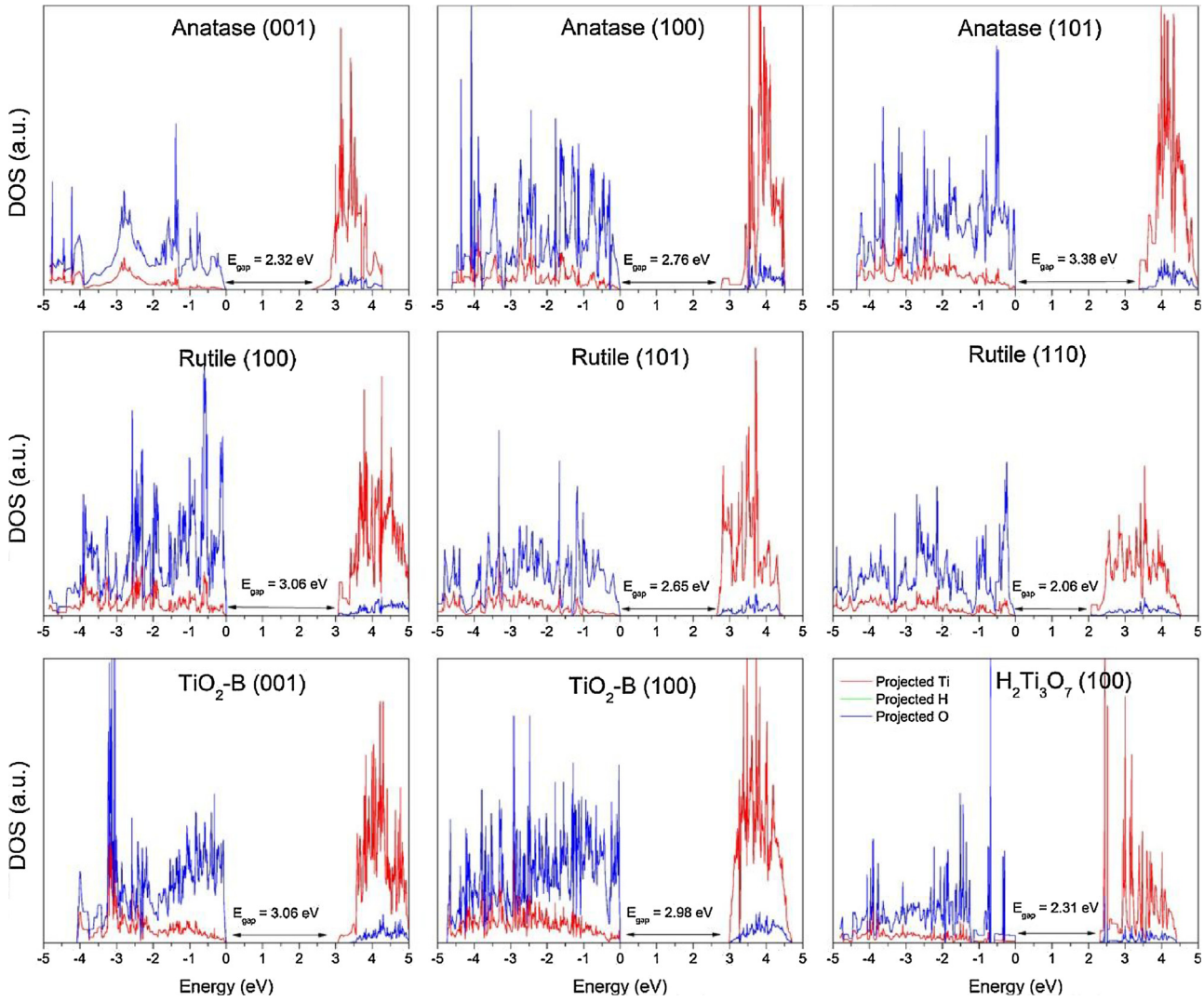

Fig. 2. Projected density of states curves for each surface, titanium contribution is plotted in red, oxygen in blue and hydrogen (for hydrogen titanate) in green. (For interpretation of the references to colour in this figure legend, the reader is referred to the web version of this article.)

avoid this error, the GGA + U approach proposed by Dudarev et al. [37] was used. Thus, the multiple occupation of *d*-orbitals is penalized, and the band gap underestimation is attenuated as well as the electron delocalization.

We can find several DFT + U studies for rutile and anatase for bulks and surfaces. Other authors have tested these U term from 3 to 10 eV [48–53]. Here we have fitted the U parameter differently depending on the polymorph under study, namely U = 8 eV for anatase, U = 10 eV for rutile, U = 4 eV for TiO_2-B and U = 5 eV for hydrogen titanate for the 3*d* levels of titanium. In a previous work −currently article in draft −, we analyzed the changes in band gap and lattice parameters for a set of U parameters, i.e. U = 3, 4, 5, 8, 10 for anatase, rutile, TiO_2-B and hydrogen titanate bulks. It was found that these selected parameters provide a good description for electronic and geometric structures.

As it can be seen in Fig. 1, the surfaces were modeled by transformation of unit cell and application of a vacuum region, along the non-periodical direction. We have selected the following surfaces: anatase (001), (100) and (101), rutile (100), (101) and (110), TiO_2-B (001) and (100) and hydrogen titanate (100). A fully slab relaxation was allowed. The Brillouin-zone was sampled using $4 \times 4 \times 1$ Monkhorst-Pack K-point mesh [54]. A cutoff energy of 400 eV was used for the plane-wave basis set.

In addition, work functions were obtained by calculating the difference between the potential in the middle of the vacuum layer and the Fermi energy [55,56]. Work function by definition, is the minimum energy required for losing an electron from a material to the vacuum, this information is fundamental for most of the electronic properties of such material. When this work function is small, the loss of an electron becomes easier. Depending on the crystalline orientation of surfaces, the work function is altered differently. In all our calculations we have used dipole correction [57] to avoid the effect caused by asymmetric of charges on the two sides of the slabs under study.

3. Results and discussion

3.1. Geometry optimization

Geometry optimization was performed for each surface at standard DFT and DFT + U approach. As it can be seen in Table 1, lattice parameters suffer a slight modification when U is different than zero. In the case of anatase, the parameter change is no larger than 4.9%, for rutile 6.2%, for TiO_2-B 2.2% and for hydrogen titanate 6.2%. The considerable improvement in the calculation of electronic properties worth it.

Table 4
Comparison of Work Function calculated with DFT and DFT + U for the studied surfaces.

	Work Function (eV)	
Surfaces	DFT	DFT + U
Anatase (001)	6.95	6.39
Anatase (100)	6.86	6.57
Anatase (101)	7.54	7.46
Rutile (100)	7.82	7.97
Rutile (101)	6.48	6.44
Rutile (110)	7.46	7.29
TiO_2-B (001)	7.10	7.11
TiO_2-B (100)	7.55	7.41
$H_2Ti_3O_7$	6.18	6.17

In Table 2 optimized Ti-O bond distances for each surface are listed. Here, it can be seen how the inclusion of U-parameter affects the geometry. Bulk anatase addresses Ti-O bond lengths of 1.94 and 1.99 Å (DFT) and 1.97 and 2.01 Å (DFT + U), when we consider the surfaces, predominantly superficial Ti-O bonds shorten and inner Ti-O bonds elongate in comparison with bulk distances. For bulk rutile, these bonds have distances of 1.95 and 1.98 Å (DFT) and 2.00 Å (DFT + U), and surfaces behave as those in anatase case, superficial bonds shorten and inner bonds elongate. In the case of TiO_2-B polymorph, the surfaces behave differently than previous cases, superficial bonds lengthen and inner bonds shorten. Bulk distances are 1.78, 1.90, 2.02 and 2.32 Å (DFT) and 1.79, 1.92, 2.02 and 2.30 Å (DFT + U). Bond lengths for hydrogen titanate perform as those in TiO_2-B, distances for bulk are 2.00, 1.82, 2.22, 1.74 and 1.94 Å (DFT) and 2.02, 1.83, 2.20, 1.78 and 1.97 Å (DFT + U). In spite of differences in geometry optimization, these are small and both calculation (DFT and DFT + U) share the same behavior after relaxation.

In literature some information about these bonds are reported, for rutile [7], anatase [58] and TiO_2-B [59] surfaces. So far hydrogen titanate is studied as nanotube, therefore that information cannot be directly comparable [24].

3.2. Energetic and electronic properties

The equivalent surface formation energy for each surface per unit area were calculated using the following equation:

$$E_{sup} = (E_{slab} - N_{Ti}E_{TiO2\text{-}bulk})/2S$$

as it was used in a previous work [29], where E_{slab} stands for the total energy of the slab, N_{Ti} corresponds to the number of TiO_2 units inside the slab, $E_{TiO2\text{-}bulk}$ is the total energy of the corresponding

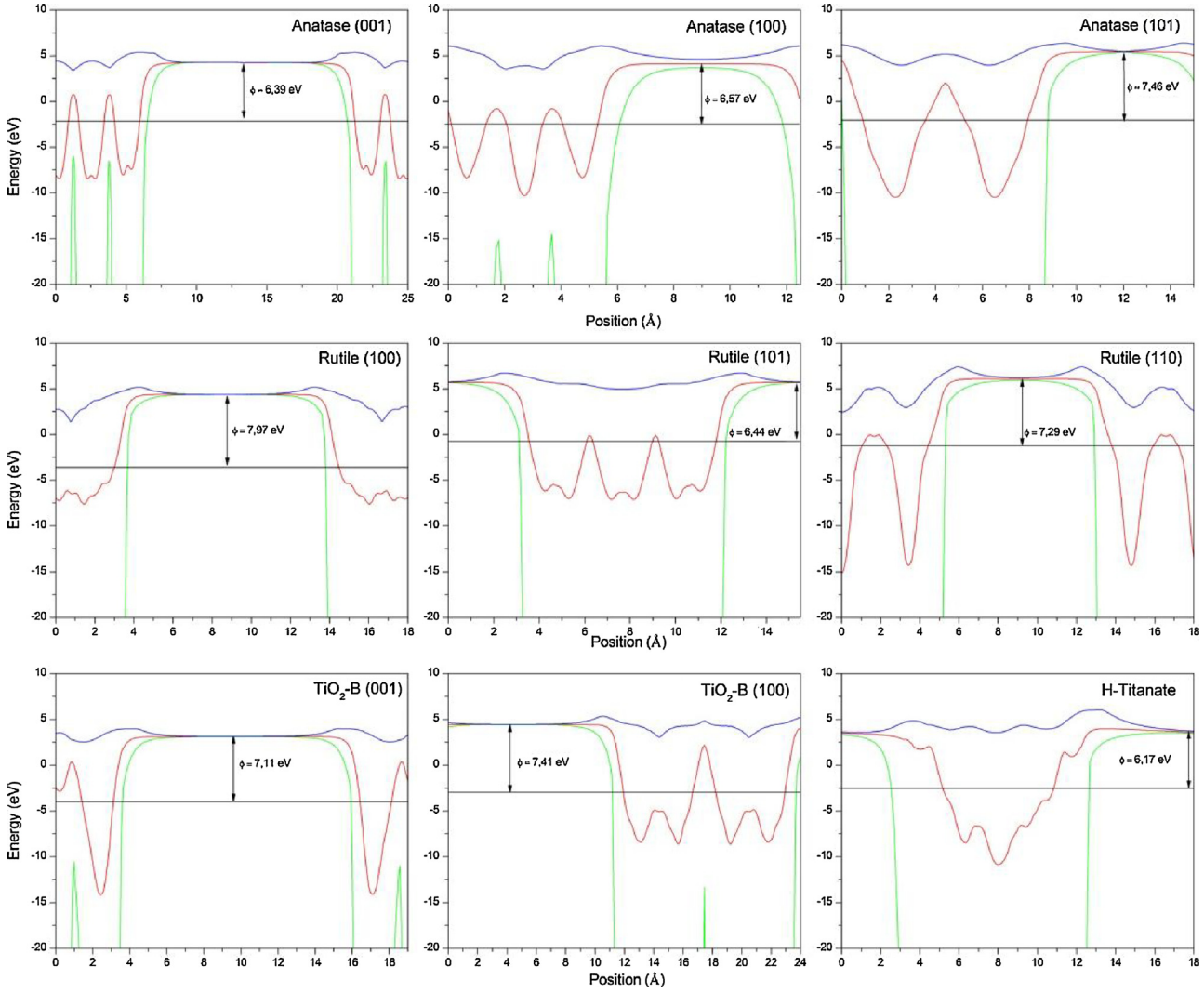

Fig. 3. Plane averaged electrostatic potential of studied surfaces. Energy vs. position in vacuum direction. Calculated by DFT + U method. Red, blue and green lines stand for averaged, maximum and minimum potential respectively. (For interpretation of the references to colour in this figure legend, the reader is referred to the web version of this article.)

bulk structure per TiO_2 unit and finally S stands for the surface area of the supercell used for the slab. The values obtained are shown in Table 3, also, by way of comparison, surface energies at U = 0 level were added. As previously expressed, in literature we can find information about anatase, rutile and TiO_2-B surface energy [6,7,29,59,60] and our results differ with those reports because unlike previous researches we have taking into account the dipole correction and the U-term, being similar the reactivity trend for each polymorph. These surface energies are sensitive to subtle changes in lattice parameters as it can be seen in the previous cited literature.

We have also reported the improvement in the calculation of energy gap when U parameter is taken into account. The experimental E_{gap} for bulk values are: 3.20 eV for anatase [61,62], 3.03 eV for rutile [62,63], 3.22 eV for TiO_2-B [64] and 3.30 eV for hydrogen titanate [65] – in the last case it is not the bulk band gap value but nanotube data-.

Band gap energies obtained using DFT + U are closer to these bulk values than calculation without U-term. In Fig. 2 projected DOS curves using DFT + U for each surface is plotted and the improved band gap indicated. In every case, the density of states shows a main contribution from oxygen 2*p* states in the valence band and an important contribution from titanium 3*d* states in the conduction band.

The characteristics of all these slabs are similar except for the value of the energy gap. This can be attributed to the shifting of the bottom of the conduction band, while the top of the valence band remains similar in every case. The bottom of the conduction band is principally composed of Ti 3*d* orbitals, for this reason the observed band gap difference depends on the contribution of these 3*d* orbitals, and it is a function of number of layers. The surface cut affects the reconstruction, Ti-O connectivity and thus the final slab properties, both electronically and structural, and in consequence TiO_2 and H-titanate final applications. For all of these reasons is not possible to establish direct and easy interpretation of the changes in the energy gaps for the same polymorph in the different cuts.

3.3. Work function

In order to obtain more information about these surfaces properties, work functions (WF) were calculated. The work function is a fundamental property of solid surfaces, which provides us with more data regarding chemical reactions, electron emission and atomic reconstruction at the surface. Titanium oxide surfaces are sensitive to the work function, to the trapping and recombination of electrons and holes in these semiconductors. The differences and singularities in each TiO_2 and hydrogen titanate surfaces will cause electrostatic fields which could affect this function [66].

In Table 4 the WF values calculated by DFT and DFT + U are listed for each surface. Differences between methods are small –from 0.22% to 4.38%. When we consider the U-term in our calculations, WF values are smaller except for R(100) and TiO_2-B(001).

We have calculated and plotted the work function for the studied surfaces as it is shown in Fig. 3. For anatase polymorph WF is found to be in the order: A(001) < A(100) < A(101); for rutile is: R(101) < R(110) < R(100); for TiO_2-B is: TiO_2-B(001) < TiO_2-B(100). Hydrogen titanate, face (001) of anatase and face (101) of rutile enhance the electron activity and the electrochemical reactivity in comparison with the remaining facets.

When comparing the WF's with the inclusion of U-term, it is observed that the WF is slightly reduced for almost all the studied surfaces, with the exception of R(100) and TiO_2-B(001) that present a slight increase in their WF values. But due to the fact that the variation is always less than a 5% we can infer that the effect of the U-term is limited and thus should not affect too much physical properties that depend on the WF.

4. Conclusion

We have performed DFT-based calculations in order to study the properties of various titanium oxides and hydrogen titanate surfaces, which are potential adsorbents in dye synthesized solar cells. Electronic properties have been improved by implementing the Hubbard term "*U*". It was found a better approximation to the experimental results in band gap energies at the expense of small deviation in optimized geometry and surface energy. Work functions of these surfaces were computed in order to have a big picture of the electronic properties.

Acknowledgments

E. G. is a member of CONICET. Authors acknowledge SGCyT (UNS), IFISUR-CONICET, CIC-Buenos Aires, PICT 1770. E. G. would like to thank Agencia Nacional de Investigación e Innovación (ANII) for providing the opportunity to undertake this research by supporting her Post-doc "Fondo Profesor Dr. Roberto Caldeyro Barcia". A. W. M. and R. F. acknowledge ANII, PEDECIBA and CSIC.

References

[1] X. Chen, S. Mao, Titanium Dioxide Nanomaterials: Synthesis, Properties, Modifications, and Applications, Chem. Rev. 107 (2007) 2891–2959.
[2] D. Chen, F. Huang, Y.-B. Cheng, R.A. Caruso, Mesoporous anatase TiO_2 beads with high surface areas and controllable pore sizes: a superior candidate for high-Performance dye-Sensitized solar cells, Adv. Mater. 21 (2009) 2206–2210.
[3] T.L. Thompson, J.T. Yates, TiO_2-based photocatalysis: surface defects, oxygen and charge transfer, Top. Catal. 35 (2005) 197–210.
[4] N. Martsinovich, D.R. Jones, A. Troisi, Electronic structure of TiO_2 surfaces and effect of molecular adsorbates using different DFT implementations, J. Phys. Chem. C 114 (2010) 22659–22670.
[5] W.-K. Li, X.-Q. Gong, G. Lu, A. Selloni, Different reactivities of TiO_2 polymorphs: comparative DFT calculations of water and formic acid adsorption at anatase and brookite TiO_2 surfaces, J. Phys. Chem. C 112 (2008) 6594–6596.
[6] A. Vittadini, M. Casarin, A. Selloni, Chemistry of and on TiO_2-anatase surfaces by DFT calculations: a partial review, Theor. Chem. Acc. 117 (2007) 663–671.
[7] H. Perron, C. Domain, J. Roques, R. Drot, E. Simoni, H. Catalette, Optimisation of accurate rutile TiO_2 (110) (100), (101) and (001) surface models from periodic DFT calculations, Theor. Chem. Acc. 117 (2007) 565–574.
[8] M. Landmann, E. Rauls, W.G. Schmidt, The electronic structure and optical response of rutile, anatase and brookite TiO_2, J. Phys.: Condens Matter 24 (2012) 195503 (6pp).
[9] S.-D. Mo, W.Y. Ching, Electronic and optical properties of three phases of titanium dioxide: rutile, anatase, and brookite, Phys. Rev. B 51 (1995) 13023–13032.
[10] D. Dambournet, I. Belharouak, K. Amine, Tailored preparation methods of TiO_2 anatase, rutile, brookite: mechanism of formation and electrochemical properties, Chem. Mater. 22 (2010) 1173–1179.
[11] D. Reyes-Coronado, G. Rodriguez-Gattorno, M.E. Espinosa-Pesqueira, C. Cab, R. de Coss, G. Oskam, Phase-pure TiO_2 nanoparticles: anatase, brookite and rutile, Nanotechnology 19 (2008) 145605 (10pp).
[12] R. Armstrong, G. Armstrong, J. Canales, R. García, R.G. Bruce, Lithium-Ion intercalation into TiO_2-B nanowires, Adv. Mater. 17 (2005) 862–865.
[13] G. Armstrong, R. Armstrong, P.G. Bruce, P. Reale, B. Scrosati, TiO_2(B) nanowires as an improved anode material for lithium-Ion batteries containing $LiFePO_4$ or $LiNi_{0.5}Mn_{1.5}O_4$ cathodes and a polymer electrolyte, Adv. Mater. 18 (2006) 2597–2600.
[14] C.C. Tsai, Y.Y. Chu, H. Teng, A simple electrophoretic deposition method to prepare TiO_2–B nanoribbon thin films for dye-sensitized solar cells, Thin Solid Films 519 (2010) 662–665.
[15] L. Qi, Y. Liu, C. Li, Controlled synthesis of TiO_2-B nanowires and nanoparticles for dye-sensitized solar cells, Appl. Surf. Sci. 257 (2010) 1660–1665.
[16] Z. Wang, A hybrid supercapacitor fabricated with a carbon nanotube cathode and a TiO_2–B nanowire anode, Adv. Funct. Mater 16 (2006) 2141–2146.
[17] D.V. Bavykin, F.C. Walsh, Titanate and Titania Nanotubes: Synthesis Properties and Applications, Royal Society of Chemistry, 2010.
[18] X.-L. Sui, Z.-B. Wang, C.-Z. Li, J.-J. Zhang, D.-M. Gu, Effect of pH value on $H_2Ti_2O_5/TiO_2$ composite nanotubes as Pt catalyst support for methanol oxidation, J. Power Sources 272 (2014) 196–202.

[19] Y. Dong, C. Xiong, Y. Zhang, S. Xing, H. Jiang, Lithium-titanate-nanotube-supported WO_3 for enhancing transmittance contrast in electrochromics, Nanotechnology 27 (2016) 105704 (10pp).
[20] W. Zhou, H. Liu, R.I. Boughton, G. Du, J. Lin, J. Wang, D. Liu, One-dimensional single-crystalline Ti?O based nanostructures: properties, synthesis, modifications and applications, J. Mater. Chem. 20 (2010) 5993–6008.
[21] M. Sugita, M. Tsuji, M. Abe, Synthetic inorganic ion-Exchange materials. LVIII. hydrothermal synthesis of a new layered lithium titanate and its alkali ion exchange, B. Chem. Soc. Jpn. 63 (1990) 1978–1984.
[22] K. Kataoka, N. Kijima, J. Akimoto, Ion-Exchange synthesis, crystal structure, and physical properties of hydrogen titanium oxide $H_2Ti_3O_7$, Inorg. Chem. 52 (2013) 13861–13864.
[23] A. Vittadini, M. Schirmer, M.-M. Walz, F. Vollnhals, T. Lukasczyk, H.-P. Steinrück, H. Marbach, A. Riss, M.J. Elser, B. Schürer, O. Diwald, Defects in oxygen-Depleted titanate nanostructures, Langmuir 28 (2012) 7851–7858.
[24] D. Szieberth, A.M. Ferrari, P. D'Arco, R. Orlando, Ab initio modeling of trititanate nanotubes, Nanoscale 3 (2011) 1113–1119.
[25] A. Eguía-Barrio, E. Castillo-Martínez, M. Zarrabeitia, M.A. Muñoz-Márquez, M. Casas-Cabanas, T. Rojo, Structure of $H_2Ti_3O_7$ and its evolution during sodium insertion as anode for Na ion batteries, Phys. Chem. Chem. Phys. 17 (2015) 6988–6994.
[26] R. Marchand, L. Brohan, M. Tournox, TiO_2(B) a new form of titanium dioxide and the potassium octatitanate $K_2Ti_8O_{17}$, Mater. Res. Bull. 15 (1980) 1129–1133.
[27] T.P. Feist, S.J. Mocarski, P.K. Davies, A.J. Jacobson, J.T. Lewandowski, Formation of TiO_2(B) by proton exchange and thermolysis of several alkali metal titanate structures, Solid State Ionics 28-30 (1988) 1338–1343.
[28] T.P. Feist, P.K. Davies, The soft chemical synthesis of TiO_2 (B) from layered titanates, J. Solid State Chem. 101 (1992) 275–295.
[29] L. Fernández-Werner, R. Faccio, A. Juan, H. Pardo, B. Montenegro, A.W. Mombrú, Ultrathin (001) and (100) TiO_2(B) sheets: surface reactivity and structural properties, Appl. Surf. Sci. 290 (2014) 180–187.
[30] S. Zhang, L.-M. Peng, Q. Chen, G.H. Du, G. Dawson, W.Z. Zhou, Formation mechanism of $H_2Ti_3O_7$ nanotubes, Phys. Rev. Lett. 91 (2003) 256103 (4pp).
[31] N.Y. Mostafa, M.B. Mohamed, N.G. Imam, M. Alhamyani, Z.K. Heiba, Electrical and optical properties of hydrogen titanate nanotube/PANI hybrid nanocomposites, Colloid Polym. Sci. 294 (2016) 215–224.
[32] Q. Du, G. Lu, Controllable synthesis and photocatalytic properties study of $Na_2Ti_3O_7$ and $H_2Ti_3O_7$ nanotubes with high exposed facet (010), J. Nanosci. Nanotechnol. 15 (2015) 4385–4391.
[33] L. Fernández-Werner, F. Pignanelli, B. Montenegro, M. Romero, H. Pardo, R. Faccio, A.W. Mombrú, Characterization of titanate nanotubes for energy applications, J. Energy Storage 12 (2017) 66–77.
[34] Z.-X. Shen, R.S. List, D.S. Dessau, O. Wells, B.O. Jepsen, A.J. Arko, R. Berttlet, C.K. Shih, F. Parmigiani, J.C. Huang, P.A.P. Lindberg, Electronic structure of NiO: Correlation and band effects, Phys. Rev. B: Condens. Matter Mater. Phys. 44 (1991) 3604–3626.
[35] I.V. Anisimov, J. Zaanen, O.K. Andersen, Band theory and mott insulators: hubbard U instead of stoner I, Phys. Rev. B: Condens. Matter Mater. Phys. 44 (1991) 943–954.
[36] V.I. Anisimov, I.V. Solvyev, M.A. Korotin, M.T. Czyzyk, G.A. Sawatzky, Density-functional theory and NiO photoemission spectra, Phys. Rev. B: Condens. Matter Mater. Phys. 48 (1993) 16929–16934.
[37] S.L. Dudarev, G.A. Botton, S.Y. Savrasov, C.J. Humphreys, A.P. Sutton, Electron-energy-loss spectra and the structural stability of nickel oxide: an LSDA + U study, Phys. Rev. B: Condens. Matter Mater. Phys. 57 (1998) 1505–1509.
[38] S.L. Dudarev, G.A. Botton, S.Y. Savrasov, Z. Szotek, W.M. Temmerman, A.P. Sutton, Electronic structure and elastic properties of strongly correlated metal oxides from first principles: LSDA + U, SIC-LSDA and EELS study of UO_2 and NiO, Phys. Status Solidi A 166 (1998) 429–443.
[39] A.I. Liechtenstein, V.I. Anisimov, J. Zaanen, Density functional theory and strong interactions: orbital ordering in mott-Hubbard insulators, Phys. Rev. B 52 (1995) R5467–5470.
[40] V.I. Anisimov, F. Aryasetiawan, A.I. Lichtenstein, First-Principles calculations of the electronic structure and spectra of strongly correlated systems: the LDA + U method, J. Phys. Condens. Matter 9 (1997) 767–808.
[41] C.J. Calzado, N.C. Hernández, J. Fdez, Sanz, Effect of on-site Coulomb repulsion term U on the band-gap states of the reduced rutile (110) TiO_2 surface, Phys. Rev. B 77 (2008) 045118 (10pp).
[42] M. Cococcioni, S. Gironcoli, Linear response approach to the calculation of the effective interaction parameters in the LDA + U method, Phys. Rev. B 71 (2005) 035105 (16pp).
[43] W. Kohn, L.J. Sham, Self-Consistent equations including exchange and correlation effects, Phys. Rev. 140 (1965) A1133–A1138.
[44] G. Kresse, J. Furthmuller, Efficiency of ab-initio total energy calculations for metals and semiconductors using a plane-wave basis set, Comput. Mater. Sci. 6 (1996) 15–50.
[45] G. Kresse, D. Joubert, From ultrasoft pseudopotentials to the projector augmented-wave method, Phys. Rev. B: Condens. Matter Mater. Phys. 59 (1999) 1758–1775.
[46] P.E. Blöchl, Projector augmented-wave method, Phys. Rev. B: Condens. Matter Mater. Phys. 50 (1994) 17953–17979.
[47] B. Hammer, L.B. Hansen, J.K. Nørskov, Improved adsorption energetics within density-functional theory using revised Perdew-Burke-Ernzerhof functionals, Phys. Rev. B: Condens. Matter Mater. Phys. 59 (1999) 7413–7421.
[48] S. Tosoni, H.-Y. Tiffany Chen, G. Pacchioni, A DFT study of the reactivity of anatase TiO_2 and tetragonal ZrO_2 stepped surfaces compared to the regular (101) terraces, ChemPhysChem 16 (2015) 3642–3651.
[49] E. Araujo-Lopez, L. Alcala Varilla, N. Seriani, J.A. Montoya, TiO_2 anatase's bulk and (001) surface, structural and electronic properties: a DFT study on the importance of Hubbard and van der Waals contributions, Surf. Sci. 653 (2016) 187–196.
[50] M. Curnan, J.R. Kitchin, Investigating the energetic ordering of stable and metastable TiO_2 polymorphs using DFT + U and hybrid functionals, J. Phys. Chem. C 119 (2015) 21060–21071.
[51] C.I.N. Morgade, G.F. Cabeza, Synergetic interplay between metal (Pt) and nonmetal (C) species in codoped TiO_2: A DFT + U study, Comp. Mater. Sci. 111 (2016) 513–524.
[52] Z. Hu, H. Metiu, Choice of U for DFT + U calculations for titanium oxides, J. Phys. Chem. C 115 (2011) 5841–5845.
[53] N. Kumar, P.R.C. Kent, D.J. Wesolowski, J.D. Kubicki, Modeling water adsorption on rutile (110) using van der waals density functional and DFT + U methods, J. Phys. Chem. C 117 (2013) 23638–23644.
[54] H.J. Monkhorst, J.D. Pack, Special points for Brillouin-zone integrations, Phys. Rev. B: Condens. Matter Mater. Phys. 13 (1976) 5188–5192.
[55] N.D. Lang, W. Kohn, Theory of metal surfaces: work function, Phys. Rev. B 3 (1971) 1215–1223.
[56] J.N. Muir, Y. Choi, H. Idriss, Computational study of ethanol adsorption and reaction over rutile TiO_2 (110) surfaces, Phys. Chem. Chem. Phys. 14 (2012) 11910–11919.
[57] J. Neugebauer, M. Scheffler, Adsorbate-substrate and adsorbate–adsorbate interactions of Na and K adlayers on Al(111), Phys. Rev. B 46 (1992) 16067–16080.
[58] M. Lazzeri, A. Vittadini, A. Selloni, Structure and energetics of stoichiometric TiO_2 anatase surfaces, Phys. Rev. B. 63 (2001) 155409 (9 pp).
[59] A. Vittadini, M. Casarin, A. Selloni, Structure and stability of TiO_2-B surfaces: a density functional study, J. Phys. Chem. C 113 (2009) 18973–18977.
[60] W. Liu, J-g. Wang, W. Li, X. Guo, L. Lu, X. Lu, X. Feng, C. Liu, Z. Yang, A shortcut for evaluating activities of TiO_2 facets: water dissociative chemisorption on TiO_2-B (100) and (001), Phys. Chem. Chem. Phys. 12 (2010) 8721–8727.
[61] S.P. Kowalczyk, F.R. McFeely, L. Ley, V.T. Gritsyna, D.A. Shirley, The electronic structure of $SrTiO_3$ and some simple related oxides (MgO, Al_2O_3 SrO, TiO_2), Solid State Commun. 23 (1977) 161–169.
[62] L. Kavan, M. Grätzel, S.E. Gilbert, C. Klemenz, H.J. Scheel, Electrochemical and photoelectrochemical investigation of single-Crystal anatase, J. Am. Chem. Soc. 118 (1996) 6716–6723.
[63] J. Pascual, J. Camassel, H. Mathieu, Fine structure in the intrinsic absorption edge of TiO_2, Phys. Rev. B 18 (1978) 5606–5614.
[64] G. Betz, H. Tributsch, R. Marchand, Hydrogen insertion (intercalation) and light induced proton exchange at TiO_2(B) −electrodes, J. Appl. Electrochem. 14 (1984) 315–322.
[65] X.G. Xu, X. Ding, Q. Chen, L.-M. Peng, Electronic, optical, and magnetic properties of Fe-intercalated $H_2Ti_3O_7$ nanotubes: first-principles calculations and experiments, Phys. Rev. B 73 (2006) 165403 (5 pp).
[66] A. Imanishi, E. Tsuji, Y. Nakato, Dependence of the work function of TiO_2 (Rutile) on crystal faces, studied by a scanning auger microprobe, J. Phys. Chem. C 111 (2007) 2128–2132.